

ORIGINAL ARTICLE

Individual-Level Identification of Gene Expression Associated with Volume Differences among Neocortical Areas

Jilian Fu[†], Feng Liu[†], Wen Qin, Qiang Xu, Chunshui Yu and Alzheimer's Disease Neuroimaging Initiative (ADNI)[‡]

Department of Radiology and Tianjin Key Laboratory of Functional Imaging, Tianjin Medical University General Hospital, Tianjin 300052, China

Address correspondence to Dr Chunshui Yu, Department of Radiology, Tianjin Medical University General Hospital, No. 154, Anshan Road, Heping District, Tianjin 300052, China. Email: chunshuiyu@tjmu.edu.cn.

[†]Jilian Fu and Feng Liu contributed equally to the work

[‡]A listing of ADNI investigators can be found at the Notes section

Abstract

The human cerebral cortex is the source of many complex behaviors and is a vulnerable target of various neuropsychiatric disorders, but transcriptional profiles linked to cerebral cortical volume (CCV) differences across brain areas remain unknown. Here, we screened CCV-related genes using an across-sample spatial correlation analysis in 6 postmortem brains and then individually validated these correlations in 1091 subjects with different ages and ethnicities. We identified 62 genes whose transcriptional profiles were repeatedly associated with CCV in more than 90% of individuals. CCV-related genes were specifically expressed in neurons and in developmental periods from middle childhood to young adulthood, were enriched in ion channels and developmental processes, and showed significant overlap with genes linked to brain functional activity and mental disorders. The identified genes represent the conserved transcriptional architecture of the human cerebral cortex, suggesting a link between conserved gene transcription and neocortical structural properties.

Key words: cerebral cortex, functional annotation, gene expression, magnetic resonance imaging, mental disorder

Introduction

The human cerebral cortex is composed of multiple areas with different structural and functional properties. As the sum of cell and non-cell components (CCs), the cerebral cortical volume (CCV) can be accurately quantified by structural magnetic resonance imaging (MRI). CCV variations have been associated with individual differences in complex cognitive capabilities (Elmer et al. 2014; Becker et al. 2015; Smolker et al. 2015), and different patterns of CCV changes have been reported in neuropsychiatric disorders (Whitwell et al. 2007; Lai 2013; Xiao et al. 2015). Although we know about the high heritability of structural neuroimaging measures (Joshi et al. 2011; de la Torre-Ubieta et al.

2018), we barely understand the genetic architecture accounting for regional CCV variations in the human brain.

The genetic architecture of cortical areas could be detected by investigating across-individual associations between genetic variants and neuroimaging measures. Although candidate gene analyses have identified a few genetic loci associated with CCV variations in several cortical areas (Nenadic et al. 2015; Udden et al. 2017; Xu et al. 2017), the generalization of these findings is difficult because only a few genetic variants from the whole human genome have been examined in rather small populations. To identify genetic variants associated with neuroimaging measures in an unbiased way, large-scale genome-wide association studies have been performed and have revealed a few

genetic loci associated with volumes of the whole brain, gray matter, and subcortical nuclei (Stein et al. 2012; Hibar et al. 2015; Xia et al. 2017; Elliott et al. 2018). However, none of these studies have reliably identified any genetic loci associated with CCV variations in any cortical areas, mainly due to the lack of enough samples.

Although cross-individual transcriptome–neuroimaging correlation analysis could be used to identify CCV-related genes, this type of analysis generally requires a large sample of donated brains with both transcriptomic and neuroimaging data. However, thus far, there have been no such big datasets. An alternate method is to identify CCV-related genes by investigating spatial correlations between gene transcription and CCV across cortical areas in a single or several postmortem brains (Fornito et al. 2019). For example, the Allen Human Brain Atlas (AHBA), including six postmortem brains with both transcriptomic and neuroimaging data, has been used to identify genes associated with neuroimaging measures of connectivity and myelin (Forest et al. 2017; Ritchie et al. 2018). Additionally, based on the fact that the cortical gene expression patterns are highly conserved across individuals (Hawrylycz et al. 2015), several studies have associated transcriptomic data from postmortem brains with group-averaging neuroimaging maps from other living brains and have revealed conserved gene expression linked to neuroimaging measures (Hawrylycz et al. 2015; Richiardi et al. 2015; Wang et al. 2015; Kong et al. 2017; Liu et al. 2019). The method has also been used to identify transcriptomic architecture associated with neuroimaging alterations resulting from neuropsychiatric disorders (Romme et al. 2017; Romero-Garcia et al. 2018). However, no study has explored CCV-related genes using transcriptome–neuroimaging association analysis.

In this study, we aimed to identify the CCV-related transcriptional architecture conserved across individuals, as this information could provide clues for understanding the genetic underpinnings of CCV variations between cortical areas in normal subjects and the molecular mechanisms underlying regional CCV changes in neuropsychiatric disorders. Transcriptome–neuroimaging association analysis was initially performed in six AHBA brains to screen out genes whose transcriptional profiles were correlated with CCV across neocortical samples. The reproducibility and generalization of these correlations were individually validated in 1091 subjects from four independent healthy populations with different ages and ethnicities. Only genes showing consistent correlation with CCV in more than 90% of individuals in every dataset were defined as CCV-related genes. The transcriptional properties of these genes were analyzed by tissue, cell type, and spatial-temporal specific expression analyses. The functions of these genes were annotated by gene set enrichment analysis, and their clinical significance was indicated by calculating the overlap between these genes and those involved in neuropsychiatric disorders. The data generation and analysis pipelines are shown in Figure 1.

Methods

Discovery Participants

The discovery experiment was performed in six donated brains with both transcriptome and structural MRI data from the AHBA (<http://human.brain-map.org>). A total of 3702 tissue samples were extracted from these brains with scalpel-based manual

macro-dissection and laser microdissection. Using a custom Agilent 8 × 60K cDNA array chip, microarray data of each tissue sample were obtained with approximately 60 000 probes to capture the expression of 20 783 genes. To minimize non-biological systematic biases while maintaining biological variations, normalization was applied both within and between brains by the Allen Institute for Brain Science. Three-dimensional T1-weighted structural MRI was also collected from the six donors shortly after the time of death and prior to tissue dissection.

Validation Participants

The validation experiments were implemented with structural MRI data from four independent datasets involving participants of different ages and ethnicities. Dataset 1 included 300 healthy young adults (150 females and 150 males; age range: 22–35 years old) from the Human Connectome Project (HCP) (<https://www.humanconnectome.org/study/hcp-young-adult>) (Van Essen et al. 2012; Van Essen et al. 2013). Dataset 2 included 300 healthy young Chinese individuals (CHY) (150 females and 150 males; age range: 18–30 years old). Dataset 3 included 228 healthy elderly subjects (110 females and 118 males; age range: 60–90 years old) from the Alzheimer Disease Neuroimaging Initiative (ADNI) (<http://www.adni-info.org/>) (Mueller et al. 2005a, 2005b; Jack et al. 2008). Dataset 4 included 263 healthy elderly Chinese individuals (CHE) (111 females and 152 males; age range: 40–75 years old).

AHBA Probe Selection

For the same gene, in a single tissue sample, different probes could obtain different gene expression values due to the different probe sensitivities. Thus, we chose one probe for one gene according to the following principles: (1) probes without Entrez ID were excluded; (2) when two probes were available for a gene, the one with higher average expression across tissue samples was retained; and (3) if more than two probes were accessible, the one most correlated with the others was preserved.

AHBA Tissue Sample Selection

AHBA provides anatomically precise genome-wide transcription maps of the human brain, including the neocortex, basal ganglia, hippocampus, cerebellum, and brainstem. It has been suggested that these major brain structures have large transcriptional differences (Hawrylycz et al. 2012). The inclusion of non-neocortical tissue samples would introduce biases into the transcriptional analysis. To investigate the molecular mechanisms of the CCV of the human brain without these biases, we only included neocortical tissue samples from the AHBA dataset in this study.

Mapping Tissue Samples to the Human Brain Atlas

The Montreal Neurological Institute (MNI) coordinates for tissue samples were used to map tissue samples to the brain atlas (Richiardi et al. 2015; Forest et al. 2017). Here, the Human Brainnetome Atlas was selected because it provided a fine-grained parcellation of the human brain and divided the neocortex into 210 non-overlapping areas based on the connectivity properties (Fan et al. 2016). We mapped the MNI coordinates of each neocortical tissue sample to this atlas to assign the tissue sample to its corresponding brain region. In this way, most tissue

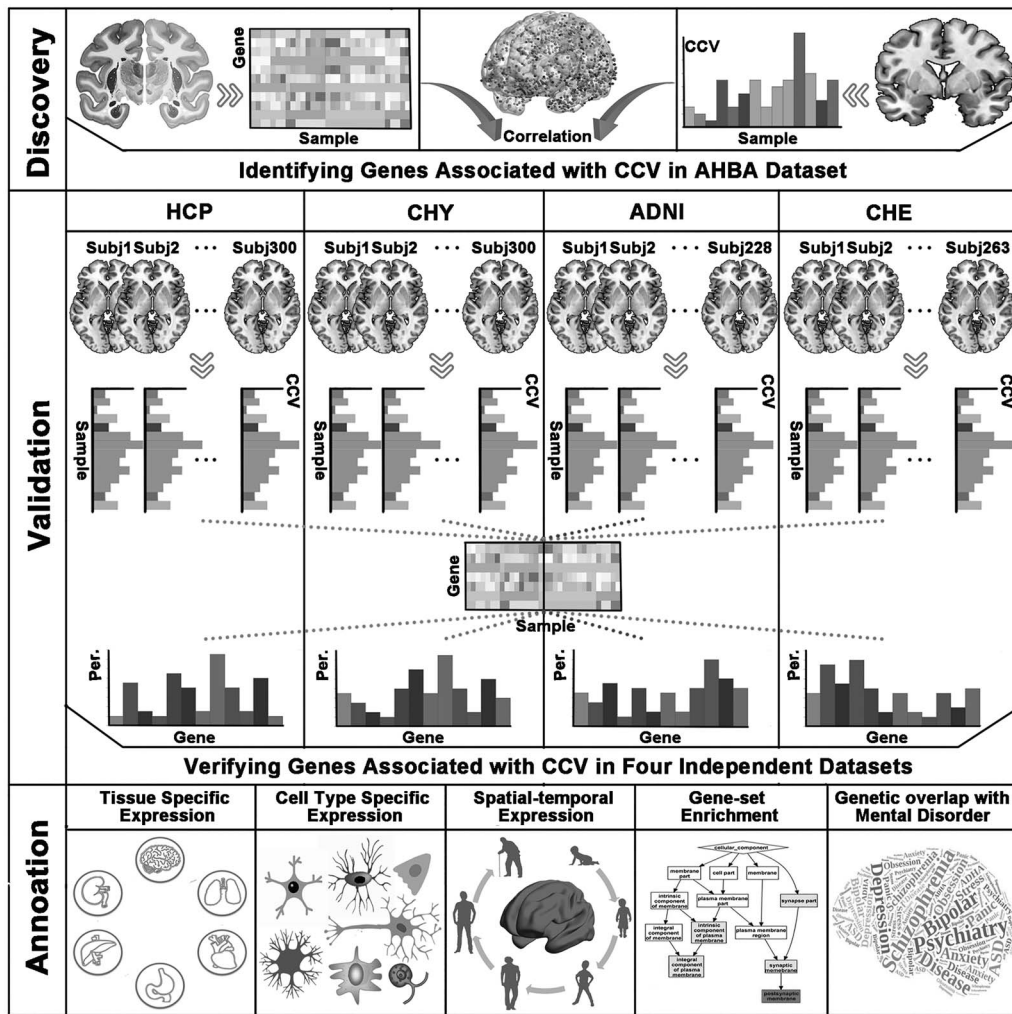


Figure 1. Data generation and analysis pipeline. This study comprises discovery experiment, validation experiment, and functional annotation. The discovery experiment is performed in six AHBA brains with both transcriptomic and structural neuroimaging data. A total of 1554 samples are assigned to the neocortex. After establishing the anatomical correspondence between transcriptomic and neuroimaging data for each sample, the CCV and gene expression (20 736 genes) of this sample are extracted. Then Pearson correlations between CCV and expression of each gene are performed across neocortical samples, and genes showing significant correlation with CCV are included in the validation experiment. The validation experiment is performed in 1091 subjects from four healthy populations with different ages and ethnicities. The expression data of the discovered genes are extracted from AHBA brains, and the CCV values of the 1554 neocortical samples are obtained from structural MRI images of each individual from the 4 datasets. Pearson correlations between CCV and gene expression are then performed across neocortical samples in each individual, and genes showing consistent significant correlation with CCV in more than 90% of individuals in every dataset are included in the annotation analysis. The identified CCV-related genes are annotated by tissue, cell type, and spatial-temporal specific expression analysis. Gene set enrichment analysis was used to identify the functions of these genes, and Fisher’s exact test was used to demonstrate the genetic overlap with mental disorders.

samples were assigned to specific brain regions. For an unmatched sample, we tested whether the sample could be mapped to the 26-connected neighboring voxels around the MNI coordinates (within a 3-voxel distance from the coordinates). If yes, the tissue sample was matched to the brain region containing the matched voxel; otherwise, the tissue sample was discarded. Finally, 1554 neocortical samples from 2748 cerebral samples provided by AHBA were matched to specific brain regions and were included in further analyses.

Imaging Data Preprocessing

We calculated a voxel-wise CCV map for each subject using the VBM8 implemented in Statistical Parametric Mapping (SPM8, <http://www.fil.ion.ucl.ac.uk/spm>). In tissue segmentation, an adaptive maximum a posteriori technique (Rajapakse et al. 1997)

and a partial volume estimation (Tohka et al. 2004) were applied to assess the fraction of each tissue type in every voxel. After the structural images were segmented into gray matter (GM), white matter, and cerebrospinal fluid, the GM concentration maps were normalized into the MNI space. The normalized CCV map was obtained by multiplying the normalized GM concentration maps by the nonlinear determinants generated from the normalization procedure. These CCV maps were resliced to a cubic voxel of 1.5 mm and smoothed with a full width at half maximum Gaussian kernel of 8 mm.

CCV Extraction for Each Sample

To establish the spatial correspondence between the CCV and gene expression for each tissue sample, we drew a sphere with a 3-mm radius on the CCV map of each individual centered on

the MNI coordinates of the tissue sample. The mean value of the CCV values of all voxels within each sphere was defined as the CCV of the tissue sample. If a sphere is extended outside the binary mask of its corresponding neocortical area, only voxels in the sphere that overlapped with the binary mask of the area were included in the calculation of the CCV of the sphere. From the CCV maps of the six donated AHBA brains, 452, 354, 149, 212, 194, and 193 spheres were extracted for each. However, all 1554 spheres (corresponding to tissue samples) were extracted for each participant in the 4 validation datasets.

Identification of the CCV-Related Genes

In the discovery experiment, both the gene expression and CCV of each neocortical sample were obtained from the same donor. Pearson correlation was performed between the CCV and the expression of each gene across all 1554 samples from all donors. Genes with significant correlations (Bonferroni correction for the number of genes) with the CCV were used for further validation analyses.

Individual-Level Validation for CCV-Related Genes

In validation experiments, gene expression was derived from the AHBA dataset, and the CCV was derived from four independent datasets. We calculated Pearson correlation coefficients for the correlation between the expression of the identified genes from the discovery experiment and the CCV of each individual from each validation dataset across all 1554 neocortical samples. Genes that were consistently significantly correlated (Bonferroni correction for the numbers of genes and subjects) with the CCV in more than 85%, 90%, and 95% of individuals in each of the four validation datasets were screened out. To balance false positive and negative rates and to increase the interpretability of the results with enrichment analyses, only genes that were consistently significantly correlated with CCV in more than 90% of individuals in each of the four validation datasets were defined as CCV-related genes and were used in the following analyses.

Permutation Test to Distinguish Significant Results from Random Results

To distinguish effective correlations from random ones, we randomly shuffled gene expression values (10000 permutations) among tissue samples and calculated correlations between the CCV and the permuted gene expression data using the same methods mentioned above. Then, we recorded the number of genes identified in each permutation test. Finally, we compared the number of genes identified in the real expression data with the number of genes identified in each permuted expression dataset to determine whether our results were different from random results.

Specificity of CCV-Related Genes to CCV

To investigate whether CCV-related genes are unique to the CCV and do not generalize to other brain structure measurements, we performed two additional tests: (1) we tested whether CCV-related genes were different from those associated with volumes of subcortical structures (SSV) and the cerebellar cortex, and (2) we tested whether CCV-related genes were also associated with cortical thickness (CT) and surface area (SA). Please see the Supplementary Methods.

Tissue-Specific Expression Analysis

We used an online tissue-specific expression analysis (TSEA) tool (<http://genetics.wustl.edu/jdlab/tsea/>) to determine the specific tissues in which CCV-related genes were overrepresented. Specifically, a specificity index probability (pSI = 0.05, 0.01, 0.001, and 0.0001, permutation corrected) was used to determine how likely a gene was to be specifically expressed in a given tissue relative to all other tissues. Fisher's exact test was used to evaluate the significance of overlap between CCV-related genes and those enriched in a particular tissue. The false discovery rate (FDR) caused by multiple comparisons was corrected using the Benjamini and Hochberg method (FDR-BH correction) with a corrected P value of 0.05.

Cell Type-Specific Expression Analysis

It has been suggested that brain-wide transcriptional variations reflect the distribution of major types of cells such as neurons, oligodendrocytes, and astrocytes (Oldham et al. 2008; Hawrylycz et al. 2012). Here, an online cell type-specific expression analysis (CSEA) tool (Dougherty et al. 2010) (<http://genetics.wustl.edu/jdlab/csea-tool-2/>) was used to identify the cell types in which the CCV-related genes were overexpressed. It should be noted that the CSEA tool employs a cell-type transcriptional dataset from the mouse brain, and thus, not all CCV-related genes could be matched to their homologs in the mouse brain. Generally, matched genes surviving a pSI (how likely a gene is to be specifically expressed in a given cell type relative to all other cell types included in the analysis) of 0.05 were classified into four main cortical cell types (neuron, astrocyte, oligodendrocyte, or immune cell), and the corresponding distribution of each cell type was depicted. If a gene was specifically expressed in more than one cell type, this gene would be included in the calculation of the distribution of both cell types. The results from CSEA analysis were further validated using another transcriptome database for seven cell types in the adult mouse brain (Zhang et al. 2014). Based on the highest FPKM (fragments per kilobase of transcript sequence per million mapped fragments) value among the seven cell types, we determined the cellular preference of expression for each matched CCV-related gene and then calculated the distribution of each cell type.

Spatial-Temporal Specific Expression Analysis

To explore the spatial-temporal expression features of CCV-related genes, we again used CSEA to investigate the transcriptional enrichment of CCV-related genes in the cerebral cortex during different developmental windows. Here, the pSI (0.05, 0.01, 0.001, and 0.0001, permutation corrected) represents how likely a gene is to be specifically expressed in a given developmental stage relative to all other stages. Besides the integral analysis of CCV-related genes, individual genes with specific cortical expression in any developmental stage under a stringent threshold (pSI = 0.0001) were also identified, and their spatial-temporal expression curves were depicted with the tool from the Human Brain Transcriptome project (Kang et al. 2011) (<http://hbatlas.org/>).

Enrichment Analyses

Conserved CCV-related genes were functionally annotated using the ToppGene portal (Chen et al. 2009) (<https://toppgene>).

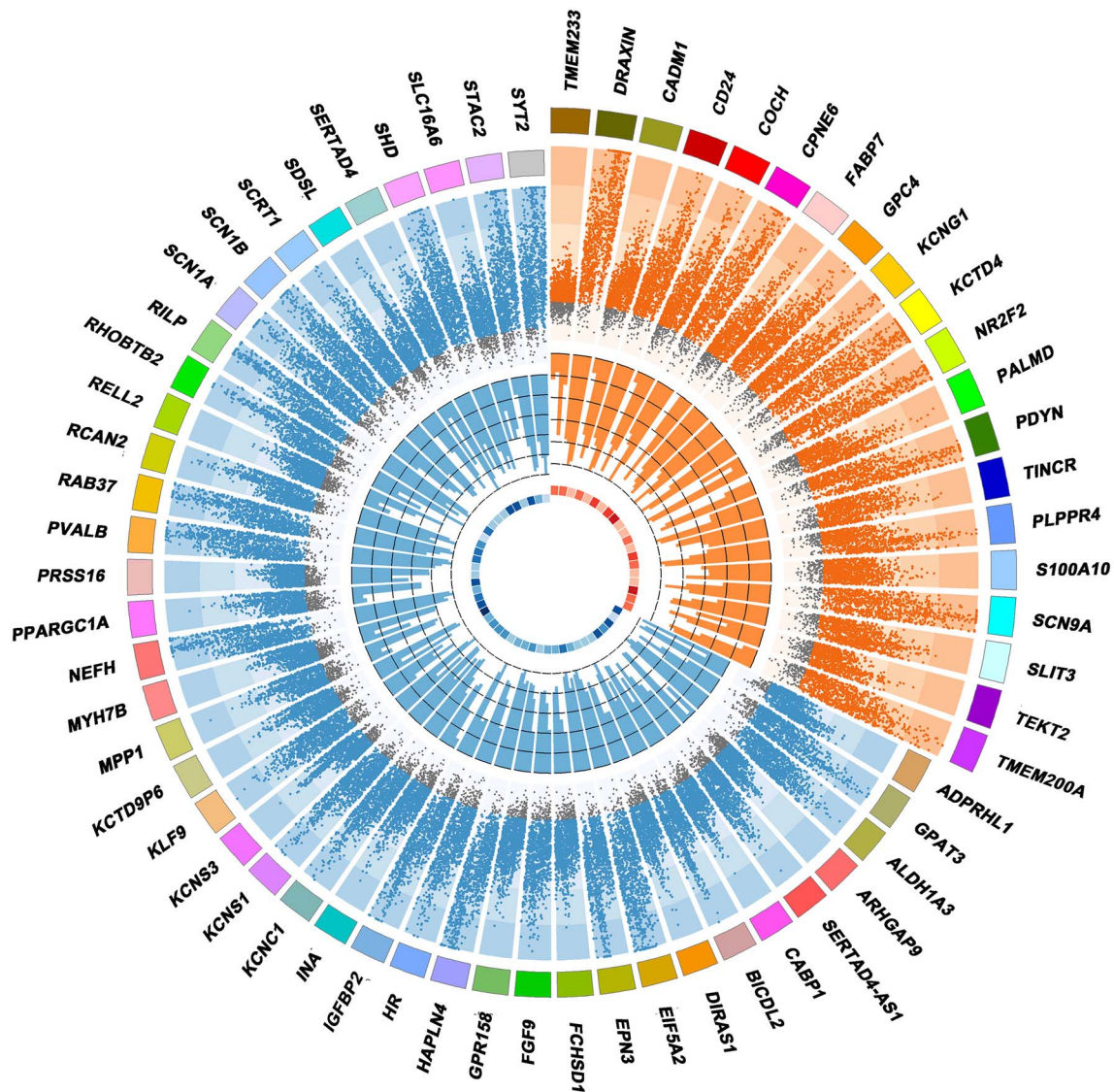


Figure 2. Genes associated with CCV. Orange represents positive correlation, and blue represents negative correlation between CCV and gene expression. The outermost ring represents $-\log_{10}(P)$ of the association test for each individual (a dot) in the validation experiment. The significant P value (Bonferroni correction) is shown in orange (positive correlation) or blue (negative correlation) dot, and the non-significant P value is shown in gray dot. The middle ring represents the percentage of consistently significant correlations in each dataset sorted clockwise as HCP, CHY, ADNI, and CHE. The black dashed circles from the outside to inside represent the probabilities of 90%, 92%, 94%, 96%, 98%, and 100%, respectively. The innermost ring represents correlation coefficient between gene expression and CCV in the discovery experiment; a darker color indicates a greater correlation coefficient (see also in [Supplementary Tables S4 and S5](#)).

cchmc.org/) to identify significant enrichment in gene ontology (GO) and human phenotype databases (FDR-BH correction, $P < 0.05$). Since major mental disorders have shown CCV changes, we also detected overlap between CCV-related genes and genes with differential expression in mental disorders. We first screened genes that survived FDR correction ($P < 0.05$) in differential expression analysis ([Gandal et al. 2018](#)), and then, we used the Fisher exact test ($P < 0.05$) to identify significant overlap between CCV-related genes and those involved in mental disorders, with 20 736 genes as the background list. The tested mental disorders included autism spectrum disorders (ASD), schizophrenia (SCZ), bipolar disorder (BD), major depression (MD), and alcohol abuse disease (AAD). We further confirmed the results using the same method, except that differentially

expressed genes (DE) were obtained from a meta-analysis of mental disorders ([Gandal et al. 2018](#)).

Statistical Analyses

The identification of CCV-related genes was performed using Pearson correlation (two-tailed) with Bonferroni correction for the number of genes ($P < 0.05/20736 = 2.41 \times 10^{-6}$). The validation of the CCV-related genes was performed using Pearson correlation (two-tailed) with Bonferroni correction for the number of genes and subjects ($P < 0.05/13784/1091 = 3.33 \times 10^{-9}$). Overlap between CCV-related genes and genes related to mental disorders was analyzed using Fisher's exact test ($P < 0.05$), with 20 736 genes as the background list.

Results

Demographic and Imaging Information of Participants

Five independent datasets were included in this study: (1) 6 postmortem brains from the AHBA with both transcriptomic and structural MRI data; (2) 300 healthy young subjects from the HCP; (3) 300 CHY; (4) 228 healthy elderly subjects from the ADNI; and (5) 263 CHE. Only structural MRI data were available for the latter four datasets. The demographic data of these datasets are shown in [Supplementary Table S1](#). The MRI parameters for these datasets are displayed in [Supplementary Table S2](#).

CCV-Related Genes Found in the Discovery Experiment

In the discovery experiment, 1554 neocortical samples were selected from a total of 3702 samples from 6 donated brains from the AHBA data. After establishing the spatial correspondence between each tissue sample and each sphere drawn from the CCV map, Pearson correlations were performed between the expression of each gene and the CCV values across all 1554 neocortical samples. We found that 13 784 of the 20 736 genes showed significant correlations with CCV (Bonferroni correction, $P < 0.05/20\,736 = 2.41 \times 10^{-6}$). The QQ plot for correlations between the CCV and gene expression is shown in [Supplementary Figure S1.A](#). We found that the observed correlations were much more significant than the expected correlations.

CCV-Related Genes Confirmed in the Validation Experiments

Individual-level validations were used to identify conserved transcriptomic architecture associated with the CCV in most individuals. We performed spatial correlations between the expression of each of the 13 784 discovered genes and the CCV values of each of the 1091 subjects from the 4 datasets including independent healthy populations with different ages and ethnicities. Genes showed a consistent correlation with the CCV in more than 85%, 90%, and 95% of individuals in every dataset, as demonstrated in [Supplementary Table S3](#). However, only genes with a consistently significant correlation with the CCV (Bonferroni correction, $P < 0.05/13\,784/1091 = 3.32 \times 10^{-9}$) in more than 90% of individuals in every dataset were defined as CCV-related genes. A total of 62 genes were identified as CCV-related genes ([Fig. 2](#), [Supplementary Figure S2](#), [Supplementary Tables S4](#) and [S5](#)). Among them, 20 genes showed positive correlations and 42 genes demonstrated negative correlations with the CCV. The representative correlation maps between gene expression levels and CCV in the discovery experiment are shown in [Figure 3](#).

Permutation Test to Distinguish Significant Results from Random Results

We randomly shuffled gene expression values (10 000 permutations) among samples and calculated correlations between the CCV and the permuted gene expression data. We found that the observed P values calculated from the permuted gene expression data are not different from the expected P values. Three representative QQ plots are shown in [Supplementary Figure S1.B–D](#). In tests with 10 000 permutations, no significant genes were found in 9806 tests, and the largest number of significant genes found in the 2 tests was 18 genes, substantially fewer than our previous finding of 62 significant

genes ([Supplementary Figure S1.E](#)). These analyses indicate that the 62 genes identified in our study are not a random result.

Specificity of CCV-Related Genes to the CCV

In the discovery experiment, 8647 genes demonstrated significant sample-wise correlations with SSV (Bonferroni correction, $P < 0.05/20\,736 = 2.41 \times 10^{-6}$). In the validation experiments, 828 genes showed consistently significant correlations with SSV (Bonferroni correction, $P < 0.05/8647/1091 = 5.30 \times 10^{-9}$) in more than 90% of individuals at each of the four validation datasets. Among the 828 genes, only three genes overlapped with 62 CCV-related genes ([Supplementary Figure S3A](#)). In addition, 6869 genes demonstrated significant sample-wise correlations with the cerebellar cortical volume (Bonferroni correction, $P < 0.05/20\,736 = 2.41 \times 10^{-6}$) in the discovery experiment. However, no genes passed the stringent threshold (Bonferroni correction, $P < 0.05/6869/1091 = 6.67 \times 10^{-9}$ in more than 90% individuals at each of the four validation datasets) in the validation experiments. These findings indicate that most of the 62 CCV-related genes are unique to the CCV and are not present in other volumes of subcortical structures and the cerebellar cortex.

We found that 2664 genes were associated with CT and that 5 genes were associated with SA. Among the 62 CCV-related genes, 58 genes overlapped with CT-related genes, but none overlapped with SA-related genes ([Supplementary Figure S3B](#)). These findings indicate that most CCV-related genes influenced cortical volume via influencing cortical thickness.

CCV-Related Genes Are Specifically Expressed in the Brain

If the transcriptome–neuroimaging association analysis is reasonable; the identified genes should show specific expression in the brain. To test this hypothesis, we used an online TSEA tool to identify the specific tissue in which CCV-related genes were significantly overrepresented. The pSI (0.05, 0.01, 0.001, and 0.0001) was applied to determine how likely a gene was to be specifically expressed in a given tissue relative to all other tissue in the analyses. We found that CCV-related genes were significantly enriched in brain tissue, even under the most stringent pSI threshold of 0.0001 ([Fig. 4A](#)). According to tissue-specific expression results at the threshold of pSI=0.05 ([Supplementary Figure S4](#)), we identified 23 brain-specific genes with specific expression in brain tissue and 10 tissue-shared genes without specific expression in any tissues ([Supplementary Figure S5A](#)) and compared correlation coefficients between brain-specific genes and tissue-shared genes. We found that brain-specific genes showed a weaker negative correlation ($t = -1.142$, $P = 0.022$) and a similar positive correlation ($t = 2.424$, $P = 0.269$) than tissue-shared genes (see [Supplementary Methods](#), [Supplementary Figure S5B](#)). These findings indicate that both brain-specific genes and tissue-shared genes are important for the CCV.

CCV-Related Genes Are Specifically Expressed in Neurons

To show the cell type-specific expression of CCV-related genes, we depicted the distribution of these genes with their specific expression (pSI=0.05, a gene is specifically expressed in a given cell type relative to all other cell type in the analyses)

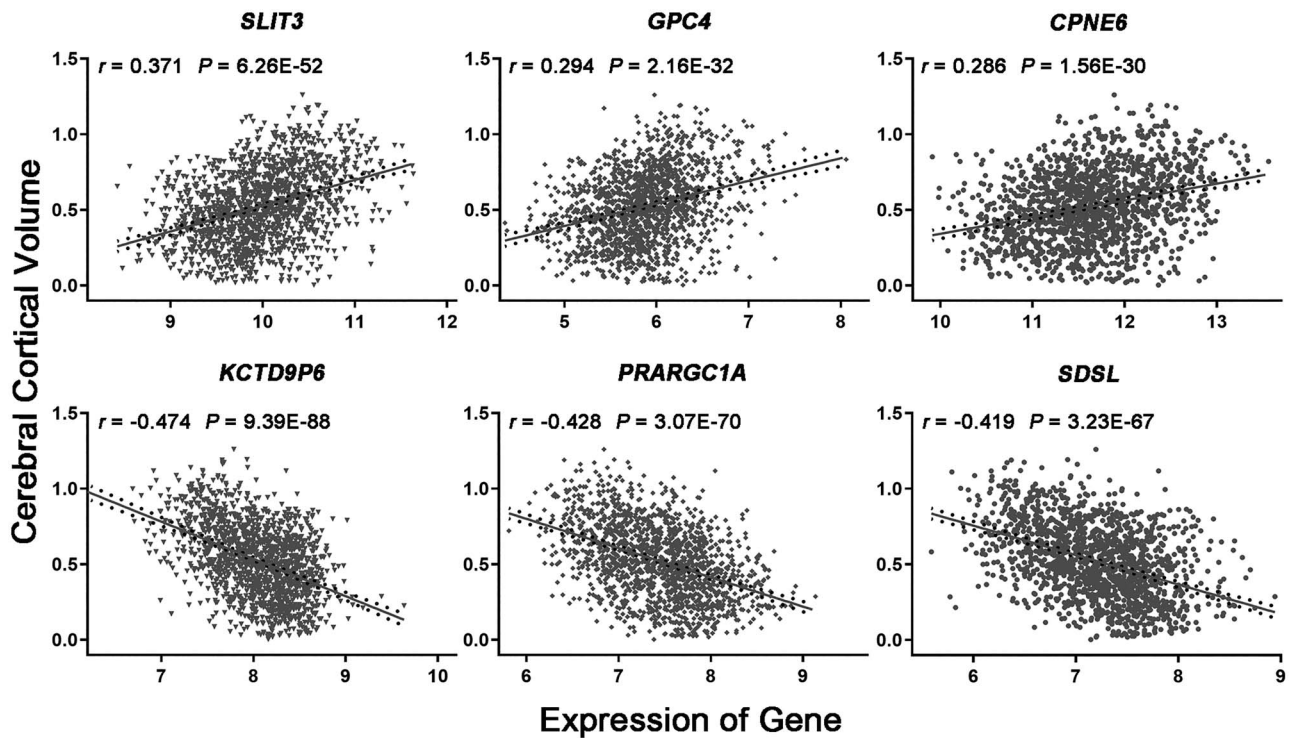


Figure 3. Correlations between gene expression and cerebral cortical volume (CCV). This figure shows three representative positive correlations (upper row) and three representative negative correlations (lower row) between gene expression and CCV across the 1554 neocortical samples in the discovery experiment (see also in [Supplementary Tables S4 and S5](#)).

in four main cortical cell types using an online CSEA tool (Dougherty et al. 2010; Xu et al. 2014). Notably, 53% of the genes showed significant specific expression in neurons (Fig. 4B and [Supplementary Table S6A](#)). We also used another transcriptome database containing seven cell types in the adult mouse brain (Zhang et al. 2014) to validate the results derived from the CSEA tool. Based on the highest FPKM value among the seven cell types, we found that 48% of CCV-related genes were preferentially expressed in neurons (Fig. 4B and [Supplementary Table S6B](#)). These findings suggest that these genes may affect the CCV by modulating cortical neurons.

CCV-Related Genes Are Specifically Expressed in the Middle and Late Developmental Stages of the Cerebral Cortex

We used CSEA to explore the enrichment of CCV-related genes in different developmental windows of the cerebral cortex. In the integral spatial-temporal specific expression analysis, these genes showed significant overexpression in middle and late childhood, adolescence, and young adulthood (Fig. 4C), suggesting that CCV-related genes are critical for the middle and late stages of cortical development. In addition to the integral analysis, the spatial-temporal specific expression of individual gene was also examined (Fig. 4D). With a strict threshold of the temporal-specific expression ($pSI=0.0001$, determines how likely a gene is to be specifically expressed in a given developmental stage relative to all other stages), CABP1, KCNS1, and STAC2 genes consistently showed gradually increased expression levels from birth to adulthood.

CCV-Related Genes Are Enriched in Brain-Related Molecular Functions, Development Processes, CCs, Functional Neuroimaging, and Disease Phenotypes

To characterize the biological functions of CCV-related genes, the ToppGene portal (Chen et al. 2009) was used to identify significant enrichment in GO and human phenotypes. The results of enrichment analyses of CCV-related genes are listed in [Supplementary Table S7](#) and are shown in [Figure 5A](#). In GO molecular functions, CCV-related genes were enriched in various ion channels, including voltage-gated ion channel ($P=0.0004$), voltage-gated sodium channel ($P=0.002$), and voltage-gated potassium channel ($P=0.006$). In GO biological processes (BPs), these genes were overrepresented in multiple development processes of the brain, such as central nervous system development ($P=0.023$), forebrain development ($P=0.023$), and head development ($P=0.033$). In GO cellular components, these genes were enriched in neurons, axons, and a variety of ion channel complexes, such as neuron part ($P=0.009$), main axon, ($P=0.002$) and sodium channel complex ($P=0.001$). In human phenotypes, these genes were enriched in many kinds of seizures, such as focal clonic seizures ($P=0.0005$), atypical absence seizures ($P=0.003$), and generalized tonic-clonic seizures with focal onset ($P=0.002$), which is consistent with the concept that primary seizures are typically caused by abnormal cortical development (Petit et al. 2014; Hsieh et al. 2016).

With transcriptomic data, several studies have revealed genes associated with functional MRI measures (Richiardi et al. 2015; Wang et al. 2015). We also examined overlap between the identified CCV-related genes and those associated with functional MRI measures, and we found significant overlap. For

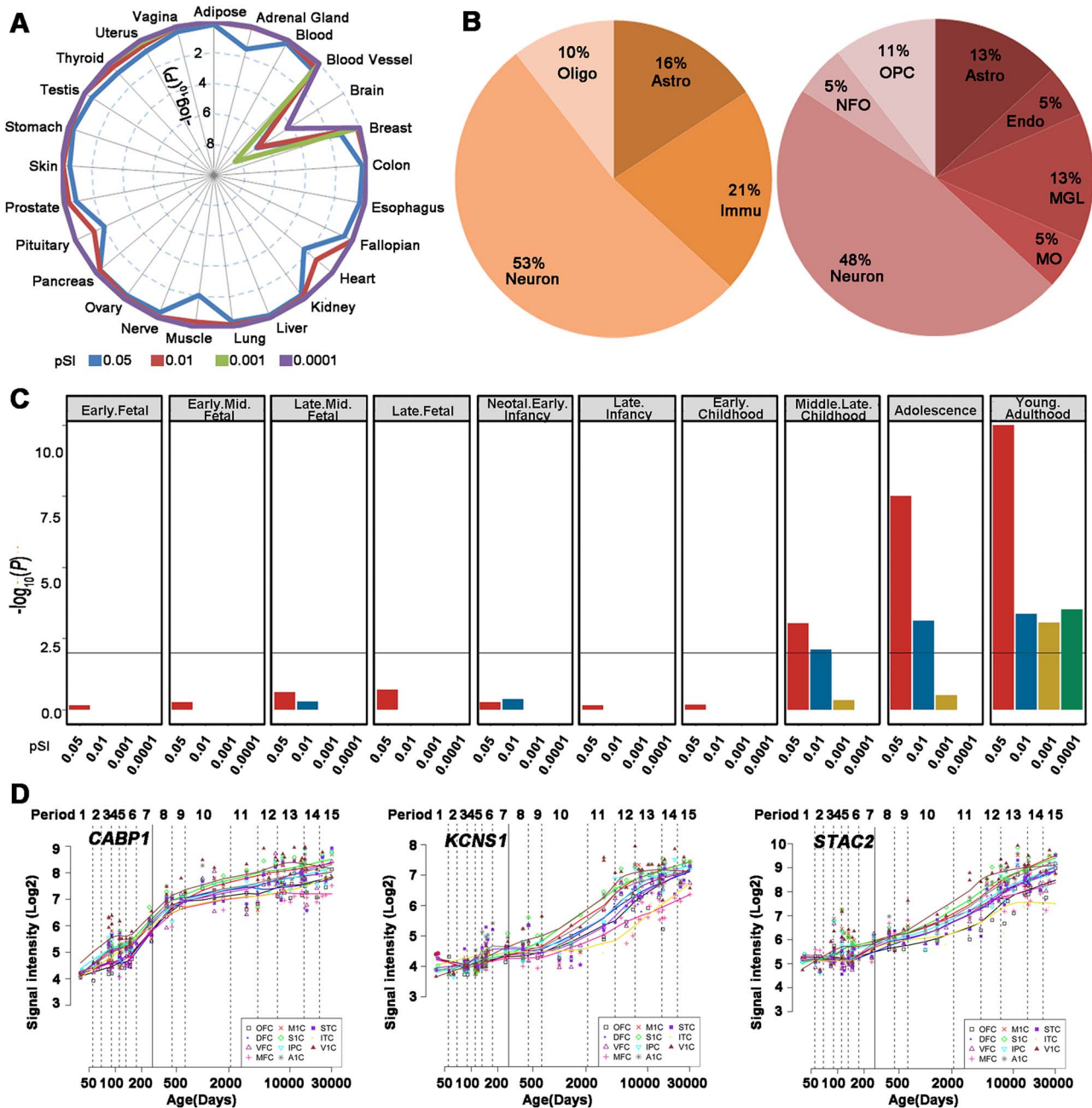


Figure 4. Specific expression analyses of the CCV-related genes. (A) Integral tissue-specific expression analysis shows that the CCV-related genes are specifically expressed in the brain rather than other tissues (pSI=0.05, 0.01, 0.001, and 0.0001). Dashed circles are $-\log_{10}(P)$ values representing the statistical significance of specific expression in different tissues. (B) Cell type-specific expression analysis indicates that the CCV-related genes are overexpressed in neurons under a threshold of pSI=0.05 in CSEA tool (left pie) and based on the highest RPKM value among the seven cell types (right pie) (see also in [Supplementary Table S6A,B](#)). (C) Integral spatial-temporal specific expression analysis reveals that the CCV-related genes are specifically expressed in the cerebral cortex during middle and late childhood, adolescence, and young adulthood. Y axis is $-\log_{10}(P)$; if $-\log_{10}(P) > 10$, then $-\log_{10}(P) = 10$. (D) The spatial-temporal specific expression curves of the CABP1, KCNS1, and STAC2 genes. Astro, astrocyte; Endo, endothelial cells; Immu, immune cells; MGL, microglia; MO, myelinating oligodendrocytes; OPC, oligodendrocyte precursor cell; Oligo, oligodendrocyte.

example, 10 of the CCV-related genes ($P = 8.48 \times 10^{-12}$, Fisher's exact test) (Fig. 5C and [Supplementary Table S8](#)) overlapped with those involved in the resting-state network (Richiardi et al. 2015), and 12 of the CCV-related genes ($P = 4.20 \times 10^{-22}$, Fisher's exact test) (Fig. 5C and [Supplementary Table S8](#)) overlapped with those linked to resting-state brain activity (Wang et al. 2015). These results indicate that some CCV-related genes are

also associated with the functional properties of the cerebral cortex.

Since CCV changes have been found in many mental disorders, such as SCZ and ASD (Ecker et al. 2015; Xiao et al. 2015), we also examined overlap between CCV-related genes and DE in these mental disorders (Gandal et al. 2018). Fisher's exact test indicated that CCV-related genes significantly

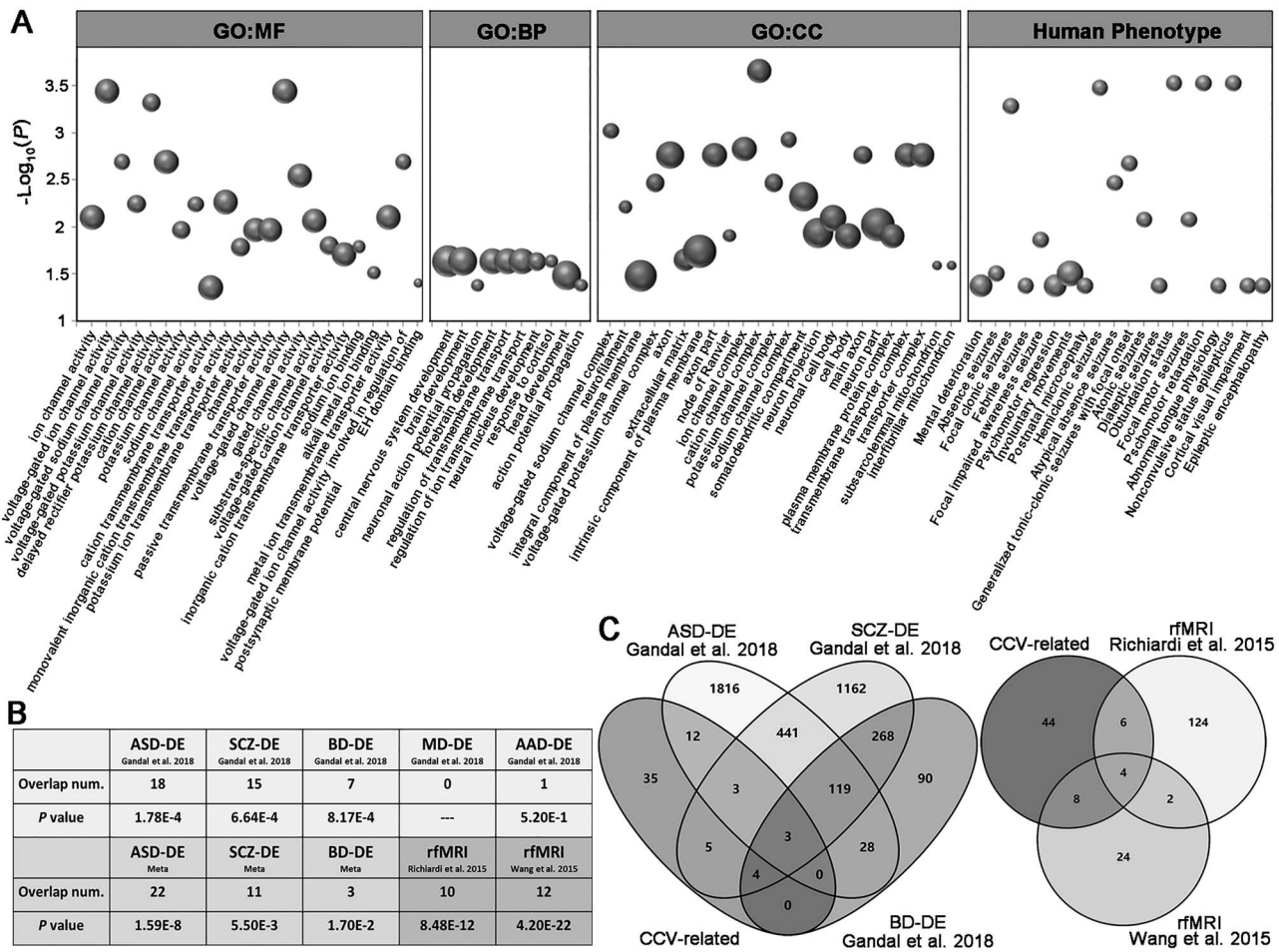


Figure 5. Functional annotations of the CCV-related genes. (A) The CCV-related genes are significantly enriched in molecular function (MF) of ion channels (left), BP of brain development (middle left), and human phenotype of seizure (right). The y axis indicates $-\log_{10}(P)$ (FDR-BH correction), and the size of each bubble depends on the number of the CCV-related genes overlapped with each gene set (see also in [Supplementary Table S7](#)). (B) The CCV-related genes are significantly overlapped with those linked to ASD, SCZ, BD, and resting-state functional magnetic resonance imaging (rfMRI) measures. (C) The numbers of the CCV-related genes overlapped with those linked to major mental disorders (left) and rfMRI measures (right).

overlapped with DE in ASD ($P=0.0002$), SCZ ($P=0.0007$), and BD ($P=0.0008$) (Fig. 5B,C and [Supplementary Table S8](#)). We also used meta-results of the DE in ASD, BD, and SCZ (Gandal et al. 2018) to validate this overlap. CCV-related genes still overlapped with those of ASD ($P=1.59 \times 10^{-8}$), SCZ ($P=0.006$), and BD ($P=0.017$) (Fig. 5B and [Table S8](#)). These results suggest that some CCV-related genes are involved in mental disorders.

Discussion

Transcriptome–neuroimaging association analysis of the whole brain is an unbiased approach to identify genes linked to neuroimaging measures. However, the reliable identification of genes associated with interindividual differences of neuroimaging measures generally requires a large sample of donated brains with both transcriptomic and neuroimaging data and with good anatomical coverage. Due to the lack of such data, researchers have investigated transcriptome–neuroimaging associations across brain areas in a few donated brains (Forest et al. 2017; Ritchie et al. 2018). Moreover, several studies have associated the transcriptomic data from postmortem brains with group-averaged neuroimaging maps from other living

brains to identify the conserved gene expression linked to neuroimaging measures (Richiardi et al. 2015; Whitaker et al. 2016; Romme et al. 2017; Shin et al. 2017; Wong et al. 2018). Here, transcriptome-CCV association analysis was initially performed in six donated brains with both types of data to avoid the strange results that can occur in association analysis based on transcriptomic and neuroimaging data from different individuals. Then, we performed stringent individual-level validation in 1091 subjects from 4 independent populations with different ages and ethnicities to ensure our findings were highly generalizable to other individuals. Thus, the identified CCV-related genes represent the conserved transcriptomic architecture accounting for CCV variations between cortical areas. However, non-conserved genes associated with CCV variations between cortical areas and genes linked to CCV variations between individuals cannot be reliably identified in this study.

Both the plausibility and significance of this study were confirmed by functional annotations of the identified CCV-related genes. These annotations showed highly specific expression in the brain and significant enrichment in neurons and axons, and nearly half of these genes showed specific expression in

neurons, which underscores the importance of neurons in mediating the effects of these genes on the CCV. These genes showed temporal-specific overexpression in the neocortex in middle and late childhood, adolescence, and young adulthood, suggesting that they are critical for the middle and late development of the cerebral cortex. For example, *CABP1*, *KCNS1*, and *STAC2* genes showed the lowest expression levels before birth, and then, these levels gradually increased with age until adulthood; these three genes have been linked to ion channels and are functionally associated with the development of and signal transduction in the brain (Moody and Bosma 2005; Hull and Isom 2018). The associations between CCV-related genes and brain development and ion channels were also confirmed by enrichment analyses. Considering the close relationship between ion channels and brain development (Moody and Bosma 2005; Hull and Isom 2018), our findings indicate that these genes may modulate cortical development via influencing ion channels.

Consistent with the well-known concept that the structure is the foundation of the function of the brain, we found significant overlap between conserved CCV-related genes and those associated with functional neuroimaging measures (Richiardi et al. 2015; Wang et al. 2015). For example, *NEFH* and *SCN1B* genes were discovered in all three studies. *NEFH* encodes the heavy chain of the neurofilament protein (a common biomarker of neuronal damage), and its mutations are associated with amyotrophic lateral sclerosis characterized by motor neuron damage (Figlewicz et al. 1994). *SCN1B* encodes the $\beta 1$ subunit of the voltage-gated sodium channel, which plays a critical role in neuronal proliferation, migration, and pathfinding (Brackenbury et al. 2013). Mutations in this gene are associated with generalized epilepsy (Robyn et al. 1998), a common brain disorder linked to the structural and functional abnormalities of neurons.

The clinical significance of CCV-related genes was further confirmed by enrichment analyses. These genes showed significant enrichment in various seizures characterized by a group of neurons firing in an abnormal, excessive, and synchronized manner (Huff and Fountain 2011). These findings could be explained by functional associations of these genes with ion channels and cortical development, abnormalities of which are important causes of seizures (Berkovic et al. 2006). We also found significant overlap between CCV-related genes and those associated with major mental disorders, such as ASD, SCZ, and BD. These findings indicate that the CCV may be a candidate intermediate phenotype for the association between these genes and mental disorders, which is consistent with previous findings showing CCV changes in these mental disorders (Ecker et al. 2015; Xiao et al. 2015). For example, the *PVALB* gene was correlated with both brain structure (CCV) and function (resting-state activity) and major mental disorders (ASD, SCZ, and BD), which is in line with the previously reported role of this gene in brain development (Kuchukhidze et al. 2015) and mental disorders (Chung et al. 2016).

Supplementary Material

Supplementary material is available at *Cerebral Cortex* online.

Funding

National Key Research and Development Program of China (2018YFC1314301); Natural Science Foundation of China (81425013, 81871431 and 81701676); Tianjin Key Technology R&D Program

(17ZXMFSY00090); Natural Science Foundation of Tianjin (18JCYBJC26300, 18JCQNJC10900).

Author Contribution

J.F., F.L., W.Q., Q.X., and C.Y. designed and conceptualized the study. J.F., F.L., and W.Q. did the data analysis. J.F., F.L., W.Q., Q.X., and T.J. were responsible for data collection and preparation. C.Y. supervised the project. J.F. and C.Y. contributed to the writing of the manuscript.

Notes

We thank Professor Michael Weiner as well as the Alzheimer's Disease Neuroimaging Initiative for their data collecting and sharing. This project was funded by the Alzheimer's Disease Neuroimaging Initiative (ADNI) (National Institutes of Health Grant U01 AG024904) and DOD ADNI (Department of Defense award number W81XWH-12-2-0012). And the project is funded by the National Institute on Aging, the National Institute of Biomedical Imaging and Bioengineering. Besides the project receives various generously contributions from the following institutes: AbbVie, Alzheimer's Association; Alzheimer's Drug Discovery Foundation; Araclon Biotech; BioClinica, Inc.; Biogen; Bristol-Myers Squibb Company; CereSpir, Inc.; Cogstate; Eisai Inc.; Elan Pharmaceuticals, Inc.; Eli Lilly and Company; EuroImmun; F. Hoffmann-La Roche Ltd and its affiliated company Genentech, Inc.; Fujirebio; GE Healthcare; IXICO Ltd; Janssen Alzheimer Immunotherapy Research & Development, LLC.; Johnson & Johnson Pharmaceutical Research & Development LLC.; Lumosity; Lundbeck; Merck & Co., Inc.; Meso Scale Diagnostics, LLC.; NeuroRx Research; Neurotrack Technologies; Novartis Pharmaceuticals Corporation; Pfizer Inc.; Piramal Imaging; Servier; Takeda Pharmaceutical Company; and Transition Therapeutics. The Canadian Institutes of Health Research is providing funds to support ADNI clinical sites in Canada. Private sector contributions are facilitated by the Foundation for the National Institutes of Health (www.fnih.org). The grantee organization is the Northern California Institute for Research and Education, and the study is coordinated by the Alzheimer's Disease Cooperative Study at the University of California, San Diego. ADNI data are disseminated by the Laboratory for Neuro Imaging at the University of California, Los Angeles. Data used in this article were obtained from the Alzheimer's Disease Neuroimaging Initiative (ADNI) database (adni.loni.usc.edu). The investigators within the ADNI contributed to the design and implementation of ADNI and/or provided data but did not participate in analysis or writing of this report.

A complete listing of ADNI investigators can be found at: http://adni.loni.usc.edu/wp-content/uploads/how_to_apply/ADNI_Acknowledgement_List.pdf.

We also thank Allen Institute Brain Science for the use of Allen Human Brain Atlas available from <http://human.brain-map.org>. And we thank Human Connectome Project for their data collecting and sharing.

Conflict of Interest: The authors declare no competing interests.

References

Becker N, Laukka EJ, Kalpouzos G, Naveh-Benjamin M, Backman L, Brehmer Y. 2015. Structural brain correlates of associative memory in older adults. *Neuroimage*. 118:146–153.

- Berkovic SF, Mulley JC, Scheffer IE, Petrou S. 2006. Human epilepsies: interaction of genetic and acquired factors. *Trends Neurosci.* 29:391–397.
- Brackenbury WJ, Yuan Y, O'Malley HA, Parent JM, Isom LL. 2013. Abnormal neuronal patterning occurs during early postnatal brain development of Scn1b-null mice and precedes Hyperexcitability. *Proc Natl Acad Sci USA.* 110:1089–1094.
- Chen J, Bardes EE, Aronow BJ, Jegga AG. 2009. Toppgene suite for gene list enrichment analysis and candidate gene prioritization. *Nucleic Acids Res.* 37:W305–W311.
- Chung DW, Fish KN, Lewis DA. 2016. Pathological basis for deficient excitatory drive to cortical parvalbumin interneurons in schizophrenia. *Am J Psychiatry.* 173:1131–1139.
- de la Torre-Ubieta L, Stein JL, Won H, Opland CK, Liang D, Lu D. 2018. The dynamic landscape of open chromatin during human cortical neurogenesis. *Cell.* 172(289–304):e218.
- Dougherty JD, Schmidt EF, Nakajima M, Heintz N. 2010. Analytical approaches to RNA profiling data for the identification of genes enriched in specific cells. *Nucleic Acids Res.* 38:4218–4230.
- Ecker C, Bookheimer SY, Murphy DGM. 2015. Neuroimaging in autism spectrum disorder: brain structure and function across the lifespan. *Lancet Neurol.* 14:1121–1134.
- Elliott LT, Sharp K, Alfaro-Almagro F, Shi S, Miller KL, Douaud G. 2018. Genome-wide association studies of brain imaging phenotypes in UK Biobank. *Nature.* 562:210–216.
- Elmer S, Hanggi J, Jancke L. 2014. Processing demands upon cognitive, linguistic, and articulatory functions promote grey matter plasticity in the adult multilingual brain: insights from simultaneous interpreters. *Cortex.* 54:179–189.
- Fan L, Li H, Zhuo J, Zhang Y, Wang J, Chen L, Yang Z, Chu C, Xie S, Laird AR et al. 2016. The human Brainnetome Atlas: a new brain atlas based on connectome architecture. *Cereb Cortex.* 26:3508–3526.
- Figlewicz DA, Krizus A, Martinoli MG, Meininger V, Dib M, Rouleau GA, Julien JP. 1994. Variants of the heavy neurofilament subunit are associated with the development of amyotrophic lateral sclerosis. *Hum Mol Genet.* 3:1757–1761.
- Forest M, Iturria-Medina Y, Goldman JS, Kleinman CL, Lovato A, Oros Klein K, Evans A, Ciampi A, Labbe A, Greenwood CMT. 2017. Gene networks show associations with seed region connectivity. *Hum Brain Mapp.* 38:3126–3140.
- Fornito A, Arnatkevičiūtė A, Fulcher BD. 2019. Bridging the gap between connectome and transcriptome. *Trends Cogn Sci.* 23:34–50.
- Gandal MJ, Haney JR, Parikshak NN, Leppa V, Ramaswami G, Hartl C, Schork AJ, Appadurai V, Buil A, Werge TM et al. 2018. Shared molecular neuropathology across major psychiatric disorders parallels polygenic overlap. *Science.* 359:693–697.
- Hawrylycz M, Miller JA, Menon V, Feng D, Dolbeare T, Guillozet-Bongaarts AL, Jegga AG, Aronow BJ, Lee CK, Bernard A et al. 2015. Canonical genetic signatures of the adult human brain. *Nat Neurosci.* 18:1832–1844.
- Hawrylycz MJ, Lein ES, Guillozet-Bongaarts AL, Shen EH, Ng L, Miller JA, van de Lagemaat LN, Smith KA, Ebbert A, Riley ZL et al. 2012. An anatomically comprehensive atlas of the adult human brain transcriptome. *Nature.* 489:391–399.
- Hibar DP, Stein JL, Renteria ME, Arias-Vasquez A, Desrivieres S, Jahanshad N, Toro R, Wittfeld K, Abramovic L, Andersson M et al. 2015. Common genetic variants influence human subcortical brain structures. *Nature.* 520:224–229.
- Hsieh LS, Wen JH, Claycomb K, Huang Y, Harrsch FA, Naegele JR, Hyder F, Buchanan GF, Bordey A. 2016. Convulsive seizures from experimental focal cortical dysplasia occur independently of cell misplacement. *Nat Commun.* 7:11753.
- Huff JS, Fountain NB. 2011. Pathophysiology and definitions of seizures and status Epilepticus. *Emerg Med Clin North Am.* 29:1–13.
- Hull JM, Isom LL. 2018. Voltage-gated sodium channel beta subunits: the power outside the pore in brain development and disease. *Neuropharmacology.* 132:43–57.
- Jack CR Jr, Bernstein MA, Fox NC, Thompson P, Alexander G, Harvey D, Borowski B, Britson PJ, L. Whitwell J, Ward C et al. 2008. The Alzheimer's disease neuroimaging initiative (ADNI): MRI methods. *J Magn Reson Imaging.* 27:685–691.
- Joshi AA, Lepore N, Joshi SH, Lee AD, Barysheva M, Stein JL, McMahon KL, Johnson K, de Zubicaray GI, Martin NG et al. 2011. The contribution of genes to cortical thickness and volume. *Neuroreport.* 22:101–105.
- Kang HJ, Kawasawa YI, Cheng F, Zhu Y, Xu X, Li M, Sousa AM, Pletikos M, Meyer KA, Sedmak G et al. 2011. Spatio-temporal transcriptome of the human brain. *Nature.* 478:483–489.
- Kong XZ, Song Y, Zhen Z, Liu J. 2017. Genetic variation in S100b modulates neural processing of visual scenes in Han Chinese. *Cereb Cortex.* 27:1326–1336.
- Kuchukhidze G, Wieselthaler-Holz A, Drexel M, Unterberger I, Luef G, Ortler M, Becker AJ, Trinka E, Sperk G. 2015. Calcium-binding proteins in focal cortical dysplasia. *Epilepsia.* 56:1207–1216.
- Lai CH. 2013. Gray matter volume in major depressive disorder: a meta-analysis of voxel-based morphometry studies. *Psychiatry Res.* 211:37–46.
- Liu F, Tian H, Li J, Li S, Zhuo C. 2019. Altered voxel-wise gray matter structural brain networks in schizophrenia: association with brain genetic expression pattern. *Brain Imaging Behav.* 13:493–502.
- Moody WJ, Bosma MM. 2005. Ion Channel development, spontaneous activity, and activity-dependent development in nerve and muscle cells. *Physiol Rev.* 85:883–941.
- Mueller SG, Weiner MW, Thal LJ, Petersen RC, Jack C, Jagust W, Trojanowski JQ, Toga AW, Beckett L. 2005a. The Alzheimer's disease neuroimaging initiative. *Neuroimaging Clin N Am.* 15:869–877; xi–xii.
- Mueller SG, Weiner MW, Thal LJ, Petersen RC, Jack CR, Jagust W, Trojanowski JQ, Toga AW, Beckett L. 2005b. Ways toward an early diagnosis in Alzheimer's disease: the Alzheimer's disease neuroimaging initiative (ADNI). *Alzheimers Dement.* 1:55–66.
- Nenadic I, Maitra R, Basmanav FB, Schultz CC, Lorenz C, Schachtzabel C, Smesny S, Nöthen MM, Cichon S, Reichenbach JR et al. 2015. Znf804a genetic variation (Rs1344706) affects brain grey but not white matter in schizophrenia and healthy subjects. *Psychol Med.* 45:143–152.
- Oldham MC, Konopka G, Iwamoto K, Langfelder P, Kato T, Horvath S, Geschwind DH. 2008. Functional organization of the transcriptome in human brain. *Nat Neurosci.* 11:1271–1282.
- Petit LF, Jalabert M, Buhler E, Malvache A, Peret A, Chauvin Y, Watrin F, Represa A, Manent JB. 2014. Normotopic cortex is the major contributor to epilepsy in experimental double cortex. *Ann Neurol.* 76:428–442.
- Rajapakse JC, Giedd JN, Rapoport JL. 1997. Statistical approach to segmentation of single-channel cerebral MR images. *IEEE Trans Med Imaging.* 16:176–186.
- Richiardi J, Altmann A, Milazzo AC, Chang C, Chakravarty MM, Banaschewski T, Barker GJ, Bokde AL, Bromberg U, Büchel C et al. 2015. Brain networks. Correlated gene expression

- supports synchronous activity in brain networks. *Science*. 348:1241–1244.
- Ritchie J, Pantazatos SP, French L. 2018. Transcriptomic characterization of MRI contrast with focus on the T1-W/T2-W ratio in the cerebral cortex. *Neuroimage*. 174:504–517.
- Robyn HW, Dao WW, Rita S, Ingrid ES, Alfred LGJ, Hilary AP, Saar K, Reis A, Johnson EW, Sutherland GR et al. 1998. Febrile seizures and generalized epilepsy associated with a mutation in the Na⁺-channel B1 subunit gene *Scn1b*. *Nature Genetics*. 19:366–370.
- Romero-Garcia R, Warriar V, Bullmore ET, Baron-Cohen S, Bethlehem RAI. 2018. Synaptic and transcriptionally downregulated genes are associated with cortical thickness differences in autism. *Mol Psychiatry*. 24:1053–1064.
- Romme IAC, de Reus MA, Ophoff RA, Kahn RS, van den Heuvel MP. 2017. Connectome disconnectivity and cortical gene expression in patients with schizophrenia. *Biol Psychiatry*. 81:495–502.
- Shin J, French L, Xu T, Leonard G, Perron M, Pike GB, Richer L, Veillette S, Pausova Z, Paus T. 2017. Cell-specific gene-expression profiles and cortical thickness in the human brain. *Cereb Cortex*. 28:3267–3277.
- Smolker HR, Depue BE, Reineberg AE, Orr JM, Banich MT. 2015. Individual differences in regional prefrontal Gray matter morphometry and fractional anisotropy are associated with different constructs of executive function. *Brain Struct Funct*. 220:1291–1306.
- Stein JL, Medland SE, Vasquez AA, Hibar DP, Senstad RE, Winkler AM, Toro R, Appel K, Bartecek R, Bergmann Ø et al. 2012. Identification of common variants associated with human hippocampal and intracranial volumes. *Nat Genet*. 44:552–561.
- Tohka J, Zijdenbos A, Evans A. 2004. Fast and robust parameter estimation for statistical partial volume models in brain MRI. *Neuroimage*. 23:84–97.
- Udden J, Snijders TM, Fisher SE, Hagoort P. 2017. A common variant of the *Cntnap2* gene is associated with structural variation in the left superior occipital Gyrus. *Brain Lang*. 172:16–21.
- Van Essen DC, Smith SM, Barch DM, Behrens TE, Yacoub E, Ugurbil K, WU-Minn HCP Consortium. 2013. The Wu-Minn Human Connectome Project: an overview. *Neuroimage*. 80:62–79.
- Van Essen DC, Ugurbil K, Auerbach E, Barch D, Behrens TE, Bucholz R, Chang A, Chen L, Corbetta M, Curtiss SW et al. 2012. The Human Connectome Project: a data acquisition perspective. *Neuroimage*. 62:2222–2231.
- Wang GZ, Belgard TG, Mao D, Chen L, Berto S, Preuss TM, Lu H, Geschwind DH, Konopka G. 2015. Correspondence between resting-state activity and brain gene expression. *Neuron*. 88:659–666.
- Whitaker KJ, Vertes PE, Romero-Garcia R, Vasa F, Moutoussis M, Prabhu G, Weiskopf N, Callaghan MF, Wagstyl K, Rittman T et al. 2016. Adolescence is associated with genomically patterned consolidation of the hubs of the human brain connectome. *Proc Natl Acad Sci USA*. 113:9105–9110.
- Whitwell JL, Przybelski SA, Weigand SD, Knopman DS, Boeve BF, Petersen RC, Jack CR Jr. 2007. 3d maps from multiple Mri illustrate changing atrophy patterns as subjects progress from mild cognitive impairment to Alzheimer's disease. *Brain*. 130:1777–1786.
- Wong AP, French L, Leonard G, Perron M, Pike GB, Richer L, Veillette S, Pausova Z, Paus T. 2018. Inter-regional variations in gene expression and age-related cortical thinning in the adolescent brain. *Cereb Cortex*. 28:1272–1281.
- Xia K, Zhang J, Ahn M, Jha S, Crowley JJ, Szatkiewicz J, Li T, Zou F, Zhu H, Hibar D et al. 2017. Genome-wide association analysis identifies common variants influencing infant brain volumes. *Transl Psychiatry*. 7:e1188.
- Xiao Y, Lui S, Deng W, Yao L, Zhang W, Li S, Wu M, Xie T, He Y, Huang X et al. 2015. Altered cortical thickness related to clinical severity but not the untreated disease duration in schizophrenia. *Schizophr Bull*. 41:201–210.
- Xu J, Qin W, Li Q, Li W, Liu F, Liu B, Jiang T, Yu C. 2017. Prefrontal volume mediates effect of COMT polymorphism on interference resolution capacity in healthy male adults. *Cereb Cortex*. 27:5211–5221.
- Xu X, Wells AB, O'Brien DR, Nehorai A, Dougherty JD. 2014. Cell type-specific expression analysis to identify putative cellular mechanisms for neurogenetic disorders. *J Neurosci*. 34:1420–1431.
- Zhang Y, Chen K, Sloan SA, Bennett ML, Scholze AR, O'Keefe S, Phatnani HP, Guarnieri P, Caneda C, Ruderisch N et al. 2014. An RNA-sequencing transcriptome and splicing database of glia, neurons, and vascular cells of the cerebral cortex. *J Neurosci*. 34:11929–11947.